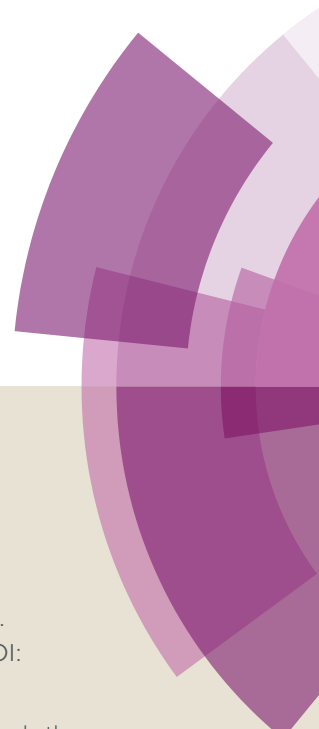
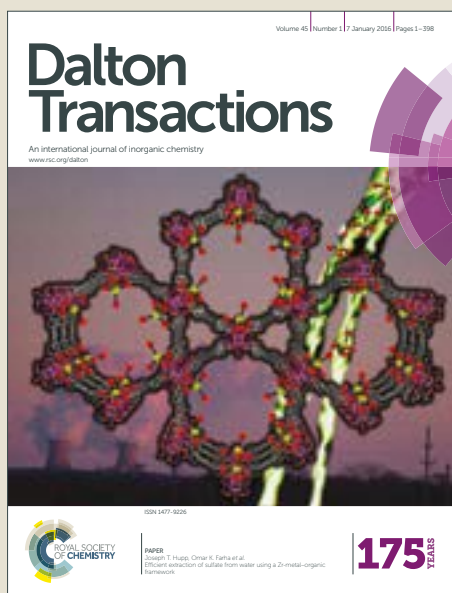


Dalton Transactions

Accepted Manuscript



This article can be cited before page numbers have been issued, to do this please use: S. Kusumoto, A. Koga, F. Kobayashi, R. Ohtani, Y. Kim, L. F. Lindoy, S. Hayami and M. Nakamura, *Dalton Trans.*, 2019, DOI: 10.1039/C9DT00593E.



This is an Accepted Manuscript, which has been through the Royal Society of Chemistry peer review process and has been accepted for publication.

Accepted Manuscripts are published online shortly after acceptance, before technical editing, formatting and proof reading. Using this free service, authors can make their results available to the community, in citable form, before we publish the edited article. We will replace this Accepted Manuscript with the edited and formatted Advance Article as soon as it is available.

You can find more information about Accepted Manuscripts in the [author guidelines](#).

Please note that technical editing may introduce minor changes to the text and/or graphics, which may alter content. The journal's standard [Terms & Conditions](#) and the ethical guidelines, outlined in our [author and reviewer resource centre](#), still apply. In no event shall the Royal Society of Chemistry be held responsible for any errors or omissions in this Accepted Manuscript or any consequences arising from the use of any information it contains.

Weak Ferromagnetism Derived from Spin Canting in an Amido-Bridged Homochiral Mn(III) 1-D Coordination Polymer

Sotaro Kusumoto,^a Atsushi Koga,^a Fumiya Kobayashi,^a Ryo Ohtani,^a Yang Kim,^a Leonard F. Lindoy,^b Shinya Hayami,^{*a,c} Masaaki Nakamura^{*a}

A homochiral one-dimensional (1D) Mn(III) coordination polymer [MnL]_n (**1**) was synthesised employing the N₃O-donor tetradentate ligand (L = 2-hydroxy-*N*-[2-[[[(2-aminophenyl)methylene]amino]-2-methylpropyl]-benzamide). The X-ray structure of **1** and its magnetic properties were investigated in detail. The crystal structure of **1** shows a homochiral helical arrangement in which spontaneous resolution has occurred, despite the ligand being achiral. Magnetic characterization revealed an antiferromagnetic interaction between manganese(III) ions ($J = -2.7 \text{ cm}^{-1}$, $g = 1.95$) that leads to an antiferromagnetic spin-ordering phase transition at $T_N \approx 7 \text{ K}$. Noteworthy, **1** exhibits weak ferromagnetism with a relatively large coercive field of 3.0 kOe based on the spin canting, indicating the formation of a homochiral weak ferromagnet.

Received 00th January 20xx,
Accepted 00th January 20xx

DOI: 10.1039/x0xx00000x

www.rsc.org/

Introduction

The study of molecular-based magnetic materials, such as single-molecule magnets (SMMs), single-chain magnets (SCMs), ferromagnets and ferrimagnets has evoked considerable interest in chemists during past decades because each of these categories has implications for the development of the next generation of quantum and molecular devices.^{1–8} For example, chiral magnetic materials that combine molecular magnetism and optical ability have attracted much attention in view of the development of multifunctional materials such as magnetochiral dichromism (MChD) and multiferroic materials.^{9–13}

The use of one-dimensional (1D) coordination polymers provides a suitable approach for the development of multifunctional materials showing both magnetism and chirality due to their often ease of design and high anisotropy. Most commonly, enantiopure ligands have been employed to introduce homochirality into coordination polymers, including by employing chiral linkers between metal centres.^{14–15} On the other hand, examples of the self-assembly of chiral coordination polymers incorporating only achiral precursors that undergo spontaneous resolution during crystallization

have also been reported.^{16–18} While syntheses of the latter type have the virtue of simplicity, unfortunately such spontaneous resolution behaviour is largely unpredictable since the associated homochiral crystal packing normally occurs serendipitously (and hence is unable to be controlled).

High-spin Mn(III) complexes are often found to behave as SMMs or SCMs, with canted behaviour and long-range magnetic order emerging because the Mn(III) ion has a large spin value ($S = 2$) and a single-ion axis anisotropy induced by the presence of a Jahn–Teller distortion on the octahedral geometry.^{19–25} In prior studies, salen-based ligands have been employed for the synthesis of 1-D Mn(III) coordination polymers in which both axial positions of the metal are occupied by various bridging ligands such as azide, cyanide and phosphonate.^{26–30} While azide-bridged systems have been used extensively for the construction of salen-derivative based magnetic systems,^{31–35} amido-bridged systems are much less common. In one study of this type, Costes and coworkers reported the synthesis and magnetic investigation of a Mn(III) complex in which a N₂O₂-donor salen derivative incorporates an amido group that acts as a bridge between Mn(III) centers to yield a 1D-chain structure showing antiferromagnetic interaction and weak ferromagnetism due to spin canting.³⁶

Motivated by the potential to obtain new magnetic coordination polymers with amido-bridges, we designed the asymmetrical N₃O-donor ligand 2-hydroxy-*N*-[2-[[[(2-aminophenyl)methylene]amino]-2-methylpropyl]-benzamide (H₃L) incorporating an amide group (Scheme 1) and synthesised the homochiral 1-D Mn(III) complex [MnL] (**1**). Spontaneous resolution of **1** occurred during crystallization from its ethanol reaction mixture and the resulting crystalline diastereomeric mixture, **1M/1P**, was isolated (and single crystals separated – see later). The magnetic characterization of **1** revealed the

^a Department of Chemistry, Graduate School of Science and Technology, Kumamoto University, 2-39-1 Kurokami, Chuo-ku, Kumamoto 860-8555, Japan. E-mail: m_nakamura@kumamoto-u.ac.jp, hayami@kumamoto-u.ac.jp

^b School of Chemistry, The University of Sydney, NSW 2006, Australia.

^c Institute of Pulsed Power Science (IPPS), Kumamoto University, 2-39-1 Kurokami, Chuo-ku, Kumamoto 860-8555, Japan.

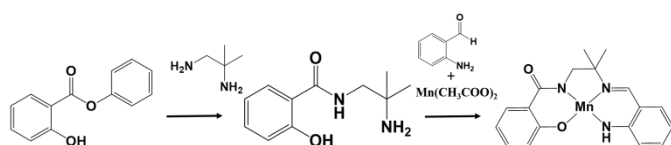
† CCDC 1862151, 1862114. For crystallographic data in CIF or other electronic format see DOI: 10.1039/x0xx00000x

existence of antiferromagnetic interactions, presumably occurring via the amido-bridges linking the metal centers ($J = -2.7 \text{ cm}^{-1}$, $g = 1.95$), as well as weak ferromagnetism caused by spin canting (ordering temperature $\approx 7 \text{ K}$). To the best of our knowledge, this represents the first report of homochiral Mn(III) amido-bridged one-dimensional coordination polymers exhibiting weak ferromagnetism.

Results and discussion

Synthesis and structural characterization

Initially, it was envisaged that H_3L might be synthesised through a straight forward two-step procedure involving the formation of a monoamide of the required diamine by reaction with phenyl salicylate followed by condensation of this intermediate with 2-aminobenzaldehyde. This second step, however, proved to be troublesome due to the tendency of 2-aminobenzaldehyde to oligomerise,³⁷ and ultimately an *in situ* procedure was employed in which $\text{Mn}(\text{OAc})_2 \cdot 4\text{H}_2\text{O}$ was added to the corresponding ligand reaction solution, leading to the mixed isomeric complexes being isolated as their Mn(III) derivatives (following aerial oxidation). Since amide ions are too strong base to exist in a solution, the deprotonation of amino group may be rationalized to occur after its coordination to the metal ion.³⁸ The dark brown colour of the products suggested that they were not Mn(II) derivatives. Elemental analyses and FT-IR spectroscopy indicated the absence of acetate anions and also that the bound ligands were triply deprotonated, in keeping with the presence of Mn(III) centres (and as established previously for related Mn(III) complexes prepared under similar conditions).³⁶ Final confirmation of the nature of the products was obtained from their single crystal X-ray structure determinations.



Scheme 1. Synthetic pathway to MnL.

[MnL] crystallizes in the lattice space group $P2_12_12_1$, indicating that the crystals are chiral (although the space group itself is not). The chirality of the crystal is associated with the conformation of the salen derivative's central chelate ring which renders each complex unit chiral (Figure 1a). 1D polymeric chains run parallel to the a axis and involve coordination of the amido-O of one complex unit to the Mn(III) centre in a neighboring unit (Figure 1b). The 1D polymer chain is helical, with the left-handed (**1M**) chain incorporating complex units in which all the central five-membered chelate rings (Mn1-N1-C8-C9-N2) have a δ conformation, whereas, all the corresponding five-membered rings in the right-handed chain have a λ conformation (Figure 2). The lattice for [MnL] viewed down the a axis (end-on to helical columns of complex units) is shown in Figure S1. The pitch of the helix is $7.856(1) \text{ \AA}$,

with the shortest intermolecular chain distance between manganese ions being 7.257 \AA . Major intermolecular interactions such as $\text{CH}\cdots\pi$, $\pi\cdots\pi$, etc. between the chains were not observed. Key bond lengths in **1M**, Mn(1)-N(1) , Mn(1)-N(2) , Mn(1)-N(3) , Mn(1)-O(1) and Mn(1)-O(2') , are $1.943(6)$, $1.991(6)$, $1.912(6)$, $1.865(4)$ and $2.119(5) \text{ \AA}$, respectively (Table 2); as expected, the bond lengths in **1P** are similar. The coordination geometry of the Mn(III) ion is best described as distorted square pyramidal, and is consistent with the presence of a Jahn-Teller distorted d^4 species; the Mn-N and Mn-O bond lengths are similar to those commonly observed for other related Mn(III) complex species.

As briefly mentioned earlier, the selection of different crystals for X-ray studies enabled the presence of both the right- and left-handed helices to be identified. For each of the crystal structures (**1M/1P**) reported here, the crystal analysed was found to be enantiomerically pure, with the value of the flack parameter having a magnitude of less than 0.023 (see Table 1). The crystals were synthesised by slow evaporation from the reaction mixture and, after allowing the solvent to evaporate to dryness in a beaker, yielded needle crystals in 'colonies' at the bottom of the beaker (Figure S2a). The solid-state CD spectra for single crystals from two colonies were determined using the KBr pellet technique (Figure S2b). The spectra were found to exhibit opposite Cotton effects, centred at about 500 nm , in accord with the formation of enantiomers via spontaneous resolution during the crystallization process. Clearly, an excess of either left-handed or right-handed enantiomer crystals occurred in the respective crystal colonies mentioned above.

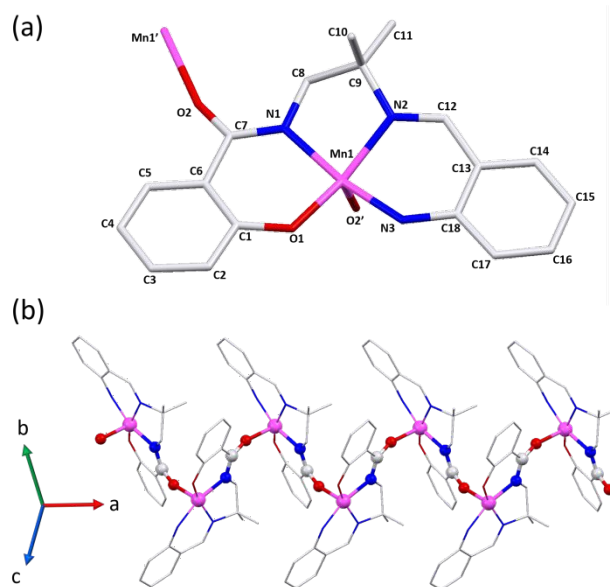


Figure 1. (a) Molecular structure of one complex unit in the **1M** coordination polymer chain. The remaining axial coordination position is filled by an amido oxygen from an adjacent unit. (b) View of the one-dimensional helical chain for **1M**. Hydrogen atoms are omitted for clarity.

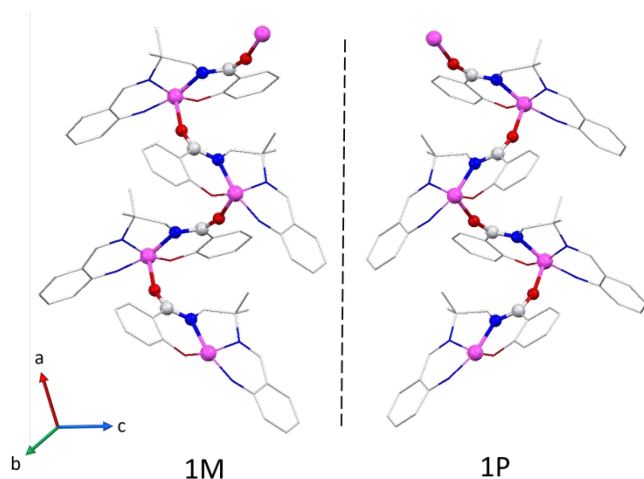


Figure 2. Mirror image relationship between the helical coordination polymers **1M** and **1P**. Hydrogen atoms are omitted for clarity.

Table 1. Crystallographic data for [MnL] (**1M** and **1P**).

Compound	1M	1P
formula	C ₁₈ H ₁₈ MnN ₃ O ₂	C ₁₈ H ₁₈ MnN ₃ O ₂
formula weight	363.29	363.30
crystal system	Orthorhombic	Orthorhombic
space group	<i>P</i> 2 ₁ 2 ₁ 2 ₁	<i>P</i> 2 ₁ 2 ₁ 2 ₁
<i>a</i> / Å	7.8555(9)	7.8586(11)
<i>b</i> / Å	11.9365(12)	11.9567(13)
<i>c</i> / Å	16.7493(14)	16.759(3)
α / °	90.0000	90.0000
β / °	90.0000	90.0000
γ / °	90.0000	90.0000
<i>V</i> / Å ³	1570.5(3)	1574.7(3)
<i>Z</i>	4	4
<i>T</i> / K	123	123
<i>D</i> _{calc} (g cm ⁻³)	1.536	1.532
<i>F</i> ₀₀₀	752.00	752.00
μ (MoK α) (cm ⁻¹)	8.561	8.538
reflns collected	13520	10267
unique data	3210	3215
parameters	14.46	14.08
<i>R</i> ₁ [<i>I</i> > 2 σ (<i>I</i>)]	0.0278	0.0579
<i>wR</i> ₂ [<i>I</i> > 2 σ (<i>I</i>)]	0.0611	0.1077
<i>R</i> ₁ (all data)	0.0319	0.901
<i>wR</i> ₂ (all data)	0.0623	0.1198
G.O.F.	1.060	0.997
Flack χ parameter	0.001(11)	-0.03(3)
CCDC	1862151	1862114

Table 2 Selected bond lengths (Å) and angles (°) for **1P/M**.

Compound	1M	1P
<i>Bond length</i>		
Mn–O1	1.860(2)	1.867(4)
Mn–N1	1.952(2)	1.945(5)
Mn–N2	1.989(2)	1.989(5)

Mn–N3	1.924(2)	1.917(5)
Mn–O2	2.124(2)	2.121(5)
<i>Angles</i>		
C7–O2–Mn1'	160.9	160.8

Magnetic properties

[Mn(L)] (**1**)

The temperature dependence of the direct-current (dc) magnetic susceptibility for the racemic mixture of **1M** and **1P** was measured in the range 2.0–300 K (Figure 3). At room temperature, the $\chi_m T$ value of 2.64 cm³ K mol⁻¹ is slightly lower than the expected value for a high-spin Mn(III) ion (3.0 cm³ K mol⁻¹, *g* = 2). Upon lowering the temperature, the $\chi_m T$ value decreases continuously and reaches a minimum of 0.357 cm³ K mol⁻¹ at 2.0 K, indicating the presence of antiferromagnetic intermolecular interactions. The magnetic interactions in the **1M** and **1P** isomers, with their similar bond length and angles (Table 2), were assumed to be equal and the experimental data were fitted based on a linear chain assuming Heisenberg isotropic coupling according to Fisher's expression for *S* = 2.³⁹ Molecular field correction was taken into account the Mean-Field Approximation as *zJ'* for the interpretation of the magnetic interaction between the chains (eqn (1)–(2)).

$$\chi = \left[\frac{Ng^2\mu^2 S(S+1)}{3k} \right] \left[\frac{1+u}{1-u} \right] \quad (1)$$

$$u = \coth \left[\frac{JS(S+1)}{kT} \right] - \left[\frac{kT}{JS(S+1)} \right] \quad (S=2)$$

$$\chi^{MFA} = \frac{\chi}{1 - \chi(zJ'/Ng^2\mu^2)} \quad (2)$$

The fit gave the following values: *J* = -2.48 cm⁻¹, *g* = 1.96, *zJ'* = -0.03 cm⁻¹. These interactions are expected to involve *dz*² orbital interactions because the *dz*² orbital has been assumed to make the main contribution to the magnetic coupling in Jahn-Teller distorted systems.³⁴

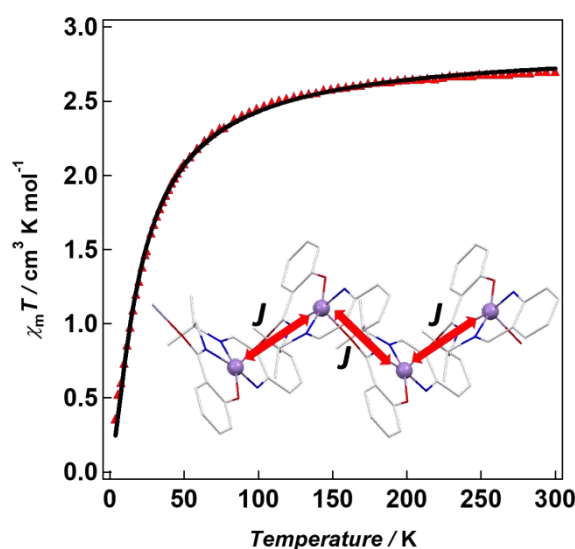


Figure 3. Temperature dependent magnetic susceptibility data for [Mn(L)]. Plots of $\chi_m T$ versus T (\blacktriangle) measured in a 5000 Oe applied field. The solid black line represents the best fit. The coupling interactions modelled are indicated by the red arrows.

Antiferromagnetic coupled 1D Mn(III) coordination polymers exhibit the possibility of exhibiting weak ferromagnetism due to spin canting, and several weak ferromagnetic azide-bridged systems of salen-based Mn(III) coordination polymers have been reported.^{31–35} The field dependence of the magnetization was measured in the range -50 kOe to 50 kOe at 2, 5 and 10 K (Figure 4a, Figure S4). At 2 K, the magnetization increases with magnetic field at low magnetic fields, while it increases slowly and in an almost linear fashion at high magnetic fields. The magnetization value reaches ca. $0.7 \text{ N}\beta \text{ mol}^{-1}$ at 50 kOe, which is far from the expected saturation value of $4.0 \text{ N}\beta \text{ mol}^{-1}$ (one Mn^{III} ion, $g = 2$ and $S = 2$). A hysteresis loop in the ordered phase with a relatively large coercive field of 3.0 kOe and a remnant magnetization of $0.0037 \text{ N}\beta \text{ mol}^{-1}$ was detected, implying the existence of canted spins (Figure S5a). The coercive field of 3.0 kOe is about ten times that of the amido-bridged 1D complex $[\text{L}^4\text{Mn}(\text{CH}_3\text{OH})]_n$ ($\text{L}^4 = (\text{E})\text{-2-hydroxy-N-(2-((2-hydroxybenzylidene)amino)ethyl)benzamide}$) reported by Costes and coworkers.³⁶ The $M(H)$ data at 2 K exhibit field-induced critical fields of around $H = 20 \text{ kOe}$, as determined by the dM/dH plot (Figure S5b). The coercive field is decreased on increasing the temperature, and the hysteresis loop measured at above the ordering temperature is completely closed, indicating the disappearance of the ordered canted spins.

The field-cooled magnetization (FCM) was measured in a field range of 1–40 kOe to confirm the spin canting (Figure 4b). During the cooling process, an abrupt rise in χ_m at around 7 K was observed under an applied field of 200 Oe, with this sharp rise in χ_m gradually vanishing on increasing the applied field. Under an applied field of larger than 7000 Oe, no such remarkable rise was observed and χ_m decreased from its maximum observed at 7 K. These behaviors are caused by a spin arrangement, demonstrating the existence of canted spins. The canting angle (α) is estimated to be $\sim 1.67^\circ$ which was calculated from $\sin^{-1}(M_w/M_s)$, where M_w is the magnetization induced by a weak magnetic field and M_s is the saturation magnetization.⁴⁰ The spin canting arises from the presence of two slanted basal planes incorporating Mn(III) ions with single ion anisotropy. The zero-field-cooled (ZFC) and field-cooled (FC) magnetization was measured under an applied field of 5 Oe (Figure 4c). Both ZFC and FC curves show abrupt increases below 7 K, indicating the occurrence of spin ordering. The temperature dependence of the ac magnetic susceptibilities at 1000 Hz (Figure 4d) exhibits the characteristic peak of an antiferromagnet at $T_N = 7 \text{ K}$, where the in-phase part χ_m' reaches a maximum; the out-of-phase χ_m'' reflection was also observed. This is indicative of long-range magnetic ordering.

Conclusions

In summary, we report here the synthesis and magnetic properties of the homochiral Mn(III) coordination polymer

[MnL] (**1**). **1** adopts a helical arrangement, with spontaneous resolution occurring on crystallization to yield isomeric homochiral left-handed and right-handed helical structures as single crystals despite both isomers being derived from an achiral free ligand. The temperature-dependent magnetic susceptibilities of **1** revealed the existence of antiferromagnetic interactions ($J = -2.7 \text{ cm}^{-1}$) occurring via the amido-bridges between Mn(III) centers. Further magnetic characterization revealed that **1** behaves as a weak ferromagnet that arises from the presence of spin canting. It is noted that the respective isomers of **1** are homochiral weak ferromagnets arising from the spin canting. As such, they represent rare examples of salen-derivative based, one-dimensional homochiral systems of this type.

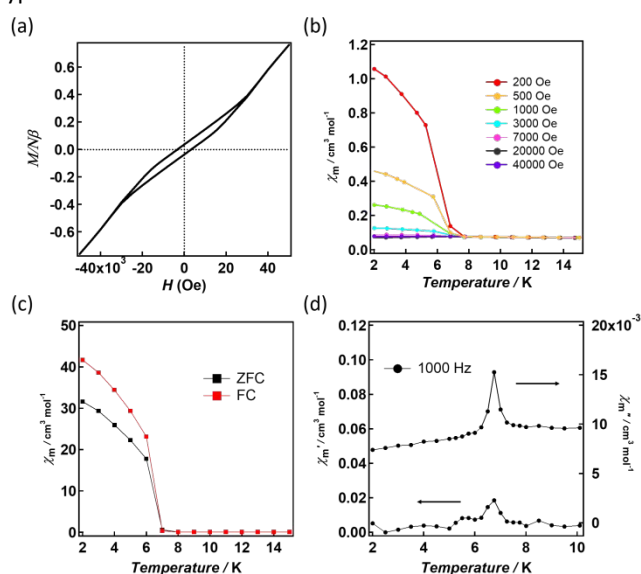


Figure 4. (a) M vs H plots at 2.0 K. (b) The χ_m vs T plots in a field range of 1–40 kOe. (c) Zero-field-cooled magnetization (ZFC) and field-cooled magnetization (FC) curves under an applied field of 5 Oe. (d) Variable-temperature in-phase (χ_m') and out-of-phase (χ_m'') components of the ac susceptibilities at 1000 Hz collected under zero dc field.

Experimental

Materials and Instruments.

All materials and reagents were commercially available and used without further purification. Elemental analyses (C, H, N) were carried out on a J-SCIENCE LAB JM10 analyzer at the Instrumental Analysis Centre of Kumamoto University. Infrared (IR) spectra were measured on a Spectrum Two FT-IR spectrometer (PerkinElmer).

Ligand Syntheses.

The synthesis of H_3L and were based on procedures previously described by us.^{41–42}

N-(2-amino-2-methylpropyl)-2-hydroxybenzamide.

Phenyl salicylate (2.14 g, 10 mmol) in 2-propanol (80 mL) was added dropwise with stirring over 1 h to a 2-propanol solution

(10 mL) containing 2-methyl-1,2-propanediamine (0.88 g, 10 mmol). The mixture was stirred for 2 days at room temperature. The resulting white precipitate was collected by filtration, washed with a small amount of 2-propanol, and dried under reduced pressure. Yield: 1.47 g (70%). Anal. calc. for $C_{11}H_{16}N_2O_2$: C, 63.44; H, 7.74; N, 13.45; Found: C, 63.46; H, 7.89; N, 13.28%. 1H NMR (500MHz, DMSO- d_6): δ 1.08 (s, 6H, CH₃), 3.26 (s, 2H, CH₂), 6.68 (t, 1H, C(5)H), 6.80 (d, 1H, C(3)H), 7.23 (t, 1H, C(4)H), 7.83 (d, 1H, C(6)H), 9.71 (l, 1H, NH). Characteristic IR absorptions: 3264, 2969, 1620, 1559, 1536 cm^{-1} .

[Mn(L)] (1)

A mixture of *N*-(2-amino-2-methylpropyl)-2-hydroxybenzamide (0.208 g, 1.00 mmol) and 2-aminobenzaldehyde (0.121 g, 1.00 mmol) in ethanol (40 mL) was stirred for 1 h at 70 °C in air. $Mn(OAc)_2 \cdot 4H_2O$ (0.245 g, 1.00 mmol) in ethanol (10 mL) was added to the resulting solution and stirring was continued for 2 h at 70 °C (also in air). **1** was obtained as a brown powder which was recrystallized from methanol to give brown needle crystals. Yield: 0.159 g (44%). Anal. calc. for $[MnL] \cdot 0.5H_2O$ ($C_{18}H_{18}MnN_3O_2 \cdot 0.5H_2O$): C, 58.09; H, 5.15; N, 11.29; Found: C, 58.30; H, 5.28; N, 11.11%. Characteristic IR absorptions: 3343, 1613, 1597, 1571, 1531 cm^{-1} .

Physical measurements

Single-crystal X-ray diffraction data for both enantiomers of **1** were obtained by selecting single crystals from different 'colonies' of crystals formed on crystallization from the reaction mixture. The data were collected with a Rigaku XtaLAB mini II diffractometer. The structures were solved by direct methods (SHELXT⁴³) and refined by full-matrix least-squares refinement using the SHELXL⁴⁴ program. Hydrogen atoms were refined geometrically using a riding model. Crystallographic data and structural refinements for **1** (both enantiomers) are summarised in Table 1. Variable-temperature dc magnetic susceptibility, ac magnetic susceptibility measurements, and field dependence of magnetization were performed on a superconducting quantum interference device (SQUID) magnetometer (Quantum Design MPMS XL). Circular dichroism (CD) spectra of KBr pellets containing the samples were measured by a JASCO J-820 spectrophotometer at RT.

Acknowledgements

This work was also supported by KAKENHI Grant-in-Aid for Scientific Research (A) JP17H01200. This work was supported by JSPS Grant-in-Aid for Young Scientists (B) JP18K14245, JSPS Grant-in-Aid for Scientific Research on Innovative Areas (Dynamical Ordering & Integrated Functions JP16H00777, Mixed Anion JP17H05485). This work was partially supported by the Cooperative Research Program of 'Network Joint Research Centre for Materials and Devices.

Conflicts of interest

There are no conflicts to declare.

References

- S. Osa, T. Kido, N. Matsumoto, N. Re, A. Pochaba and J. Mrozinski, *J. Am. Chem. Soc.*, 2004, **126**, 420–421.
- A. J. Tasiopoulos, A. Vinslava, W. Wernsdorfer, K. A. Abboud, G. Christou, *Angew. Chem. Int. Ed.*, 2004, **43**, 2117–2121.
- W.-X. Zhang, T. Shiga, H. Miyasaka, M. Yamashita, *J. Am. Chem. Soc.*, 2012, **134**, 6908–6911.
- E. Coronado, J. R. Galán-Mascarós, C. Martí-Gastaldo, *J. Am. Chem. Soc.*, 2008, **130**, 14987–14989.
- E. Coronado, J.-R. Galán-Mascarós, C. J. Gómez-García, V. Laukhin, *Nature*, 2000, **408**, 447–449.
- O. Kahn, Y. Pei, M. Verdaguer, J. P. Renard, J. Sletten, *J. Am. Chem. Soc.*, 1998, **110**, 789–792.
- S. Ferlay, T. Mallah, R. Ouahès, P. Veillet, M. Verdaguer, *Inorg. Chem.*, 1999, **38**, 229–234.
- S. M. Humphrey, P. T. Wood, *J. Am. Chem. Soc.*, 2004, **126**, 13236–13237.
- G. L. J. A. Rikken, E. Raupach, *Nature*, 1997, **390**, 493–494.
- L. D. Barron, *Nature*, 2000, **405**, 895–896.
- N. Hur, S. Park, P. A. Sharma, J. S. Ahn, S. Guha, S.-W. Cheong, *Nature*, 2004, **429**, 392–395.
- J. H. Lee, L. Fang, E. Vlahos, X. Ke, Y. W. Jung, L. F. Kourkoutis, J.-W. Kim, P. J. Ryan, T. Heeg, M. Roeckerath, V. Goian, M. Bernhagen, R. Uecker, P. C. Hammel, K. M. Rabe, S. Kamba, J. Schubert, J. W. Freeland, D. A. Muller, C. J. Fennie, P. Schiffer, V. Gopalan, E. Johnston-Halperin, D. G. Schlom, *Nature*, 2010, **466**, 954–958.
- P. Jain, V. Ramachandran, R. J. Clark, H. D. Zhou, B. H. Toby, N. S. Dalal, H. W. Kroto, A. K. Cheetham, *J. Am. Chem. Soc.*, 2009, **131**, 13625–13627.
- Crassous, J. *Chem. Soc. Rev.*, 2009, **38**, 830–845.
- Q. Zhu, T. Sheng, R. Fu, C. Tan, S. Hu and X. Wu, *Chem. Commun.*, 2010, **46**, 9001–9003.
- T. Ezuhara, K. Endo and Y. Aoyama, *J. Am. Chem. Soc.*, 1999, **121**, 3279–3283.
- I. Mihalcea, N. Zill, V. Mereacre, C. E. Anson and A. K. Powell, *Cryst. Growth Des.*, 2014, **14**, 4729–4734.
- K. K. Bisht and E. Suresh, *J. Am. Chem. Soc.*, 2013, **135**, 15690–15693.
- C. J. Milios, R. Inglis, A. Vinslava, R. Bagai, W. Wernsdorfer, S. Parsons, S. P. Perlepes, G. Christou, E. K. Brechin, *J. Am. Chem. Soc.*, 2007, **129**, 12505–12511.
- T. C. Stamatatos, D. Foguet-Albiol, S.-C. Lee, C. C. Stoumpos, C. P. Raptopoulou, A. Terzis, W. Wernsdorfer, S. O. Hill, S. P. Perlepes, G. Christou, *J. Am. Chem. Soc.*, 2007, **129**, 9484–9499.
- X. Chen, S.-Q. Wu, A.-L. Cui, H.-Z. Kou, *Chem. Commun.*, 2014, **50**, 2120–2122.
- C. Papatriantafyllopoulou, S. Zartilas, M. J. Manos, C. Pichon, R. Clérac, A. J. Tasiopoulos, *Chem. Commun.*, 2014, **50**, 14873–14876.
- C.-I. Yang, Z.-Z. Zhang, S.-B. Lin, *Coord. Chem. Rev.*, 2015, **289–290**, 289–314.
- K. Bernot, J. Luzon, R. Sessoli, A. Vindigni, J. Thion, S. Richeter, D. Leclercq, J. Larionova, A. v. d. Lee, *J. Am. Chem. Soc.*, 2008, **130**, 1619–1627.
- B. Cheng, F. Cukiernik, P. H. Fries, J.-C. Marchon, W. R. Scheidt, *Inorg. Chem.*, 1995, **34**, 4627–4639.
- T.-T. Wang, M. Ren, S.-S. Bao, B. Liu, L. Pi, Z.-S. Cai, Z.-H. Z.-H. Zheng, Z.-L. Xu, L.-M. Zheng, *Inorg. Chem.*, 2014, **53**, 3117–3125.
- T.-T. Wang, M. Ren, S.-S. Bao, Z.-S. Cai, B. Liu, Z.-H. Zheng, Z.-L. Xua, L.-M. Zheng, *Dalton Trans.*, 2015, **44**, 4271–4279.
- T. Senapati, C. Pichon, R. Ababei, Mathonière, C.; Clérac, R. *Inorg. Chem.*, 2012, **51**, 3796–3812.
- C. Yang, Q.-L. Wang, J. Qi, Y. Ma, S.-P. Yan, G.-M. Yang, P. Cheng, D.-Z. Liao, *Inorg. Chem.*, 2011, **50**, 4006–4015.

ARTICLE

Journal Name

- 30 M.-X. Yao, Q. Zheng, X.-M. Cai, Y.-Z. Li, Y. Song, J.-L. Zuo, *Inorg. Chem.*, 2012, **51**, 2140–2149.
- 31 H. H. Ko, J. H. Lim, H. C. Kim, C. S. Hong, *Inorg. Chem.*, 2006, **45**, 8847–8849.
- 32 M. Yuan, F. Zhao, W. Zhang, Z.-M. Wang, S. Gao, *Inorg. Chem.*, 2007, **46**, 11235–11242.
- 33 J. H. Yoon, J. W. Lee, D. W. Ryu, S. W. Yoon, B. J. Suh, H. C. Kim, C. S. Hong, *Chem. Eur. J.*, 2011, **17**, 3028–3034.
- 34 K. R. Reddy, M. V. Rajasekharan, J.-P. Tuchagues. *Inorg. Chem.*, 1998, **37**, 5978–5982.
- 35 J. H. Yoon, D. W. Ryu, H. C. Kim, S. W. Yoon, B. J. Suh, C. S. Hong, *Chem. Eur. J.*, 2009, **15**, 3661–3665.
- 36 J.-P. Costes, F. Dahan, B. Donnadieu, M.-J. R. Douton, M.-I. F. Garcia, A. Bousseksou, J.-P. Tuchagues, *Inorg. Chem.*, 2004, **43**, 2736–2744.
- 37 L. T. Taylor, S. C. Vergez and D. H. Busch, *J. Am. Chem. Soc.*, 1966, **88**, 3170–3171.
- 38 S. Gakias, C. Rix, A. Fowless, M. Hobday, *Inorg. Chem. Acta*, 2006, **359**, 2291–2295.
- 39 M. E. Fisher, *Am. J. Phys.*, 1964, **32**, 343.
- 40 Kahn, O. *Molecular Magnetism*; VCH: Weinheim, Germany, 1993.
- 41 S. Kusumoto, F. Kobayashi, R. Ohtani, Y. Zhang, J. Harrowfield, Y. Kim, S. Hayami, M. Nakamura, *Dalton Trans.*, 2018, **47**, 9575–9578.
- 42 F. Kobayashi, R. Ohtani, S. Teraoka, W. Kosaka, H. Miyasaka, Y. Zhang, L. F. Lindoy, S. Hayami, M. Nakamura, *Dalton Trans.*, 2017, **46**, 8555–8561.
- 43 G. M. Sheldrick, SHELXT – Integrated Space-Group and Crystal-Structure Determination. *Acta Crystallogr. Sect. A* 2015, **71**, 3–8.
- 44 G. M. Sheldrick, Crystal Structure Refinement with SHELXL. *Acta Crystallogr. Sect. C* 2015, **71**, 3–8.

View Article Online
DOI: 10.1039/C9DT00593E

Dalton Transactions Accepted Manuscript